

# Numerical Investigation on the Performance of Plate Heat Exchangers for Core and Bypass Ducts in High-Speed Micro Aero-Engines

Xingao Shu <sup>1,\*</sup>, Chen Xia <sup>1</sup>

<sup>1</sup>Nanjing University of Aeronautics and Astronautics

**Abstract.** This paper utilizes the Computational Fluid Dynamics (CFD) method to systematically investigate the influence of cold-side (Recold) and hot-side (Rehot) inlet Reynolds numbers on the heat transfer, flow performance, and thermodynamic irreversibility (entropy generation) of an annular plate heat exchanger integrated into a micro aero-engine. The research results indicate that as the cold-side Recold increases, the cold-side convective heat transfer coefficient ( $h_{cold}$ ) is significantly enhanced; however, the high-velocity fluid experiences a pressure-drop-induced expansion cooling effect in the latter half of the channel, which suppresses the gas temperature rise—this unique physical mechanism is explicitly confirmed through a comparative simulation with an incompressible fluid model. Simultaneously, increasing the hot-side Rehot significantly boosts the system's average heat transfer rate and the overall heat transfer coefficient ( $U$ ), with an exceptional growth rate of 91.13% for the average heat transfer rate when Rehot increases from 2000 to 5000. Furthermore, the entropy generation analysis shows that the cold-side Reynolds number is more sensitive to the system's total entropy production, suggesting its optimization potential is superior to that of the hot side. This study provides crucial theoretical basis and optimization guidelines for the design of high-efficiency, low-resistance heat exchangers operating under the high-Mach number conditions typical of micro aero-engines.

**Keywords:** annular plate heat exchanger; micro aero-engine; high-Mach number flow.

## 1. Introduction

Micro gas turbines are widely used in applications including unmanned aerial vehicles (UAVs). However, miniaturization introduces issues such as machining errors, leakage losses, and low Reynolds number effects, which contribute to high fuel consumption. To enhance performance, this study integrates a recuperative heat exchanger into a micro-turbofan engine, aiming to recover waste heat, improve the work capacity of the bypass flow, and achieve high bypass ratio operation [1].

An annular plate heat exchanger is adopted for its compact structure and large heat transfer area. Nevertheless, in aero-engine applications, it operates under high-speed inflow conditions (bypass  $Ma \approx 0.1$ , core  $Ma \approx 0.42$ ), significantly exceeding conventional heat exchanger flow speeds ( $Ma < 0.03$ ). High-speed flow reduces gas residence time, limiting heat transfer completeness, and increases flow resistance, thereby reducing exergy output. Resolving this trade-off between heat transfer enhancement and flow loss is essential, with the Reynolds number being the key governing parameter.

The Reynolds number critically influences both heat transfer and flow resistance. Its increase transitions the flow from laminar to turbulent, enhancing fluid mixing and heat transfer capability—for instance, raising the local heat transfer coefficient by about 80.9% in supercritical heat exchangers [2]. However, higher Reynolds numbers also lead to increased flow resistance and pressure drop, necessitating a balance between thermal efficiency and energy consumption. Existing studies show that the effect of Reynolds number on heat exchanger performance is complex. While turbulence at high Reynolds numbers improves heat transfer, it can also cause flow maldistribution and higher friction losses. For example, the friction factor decreases with Reynolds number up to  $Re = 20,000$ , but rises sharply when  $Re$  exceeds 40,000 [3]. This study employs CFD simulations to systematically investigate the effects of cold-side and hot-side inlet Reynolds numbers on the heat transfer, flow resistance, and thermodynamic performance—assessed via entropy generation—of

the annular plate heat exchanger. It aims to clarify compressible flow behavior under high-speed conditions and identify the optimal Reynolds number range from an exergy and entropy generation perspective [4], providing theoretical support for designing high-efficiency, low-resistance heat exchangers.

## 2. Numerical Model

### 2.1 Geometric Model and Mesh Generation

This study sets the characteristic diameter of the core flow channel at 340mm and the characteristic diameter of the bypass flow channel at 540mm, based on which the flow channel height of the annular plate heat exchanger is determined to be 100mm. In industrial applications, the specific surface area parameter of conventional heat exchangers is typically less than  $1000 \text{ m}^2/\text{m}^3$ . Based on the upper limit of industry benchmark parameters, this study selects a heat exchanger model with a specific surface area of  $1000 \text{ m}^2/\text{m}^3$  as the design optimization benchmark. To maintain a constant specific surface area, the system adopts a topological configuration of 300 periodic microchannel units, yielding an equivalent rectangular width of 4.6mm through geometric equivalence calculation. Considering the overall dimensional constraints and engineering practicality requirements of the heat exchanger, the axial characteristic length of the baseline model is preliminarily determined to be 500mm.[5]

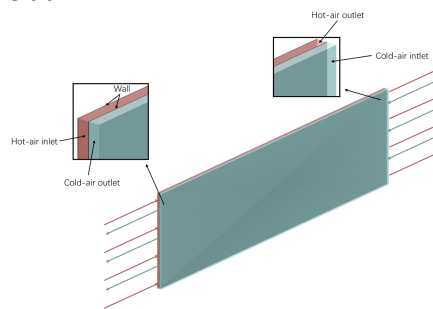


Fig. 1 Plate Heat Exchanger Model

Structured grids were generated for the straight section of the heat exchanger using ANSYS ICEM. The mesh near the walls was refined to ensure the  $y^+$  value near the wall surface was between 30 and 60. The height of the first layer of mesh was set to 0.05mm, and the growth factor in the mesh height direction was 1.2. This gradually increasing mesh size helps maintain accuracy in the near-wall region while reducing the total mesh count and lowering computational costs. A heat exchanger model with a plate spacing of 2.3mm and a length of 500mm was selected for preliminary calculations using different mesh counts. Heat exchange efficiency was used as the criterion to determine whether the mesh density met the requirements. The mesh of the straight plate section is shown in Fig.2.

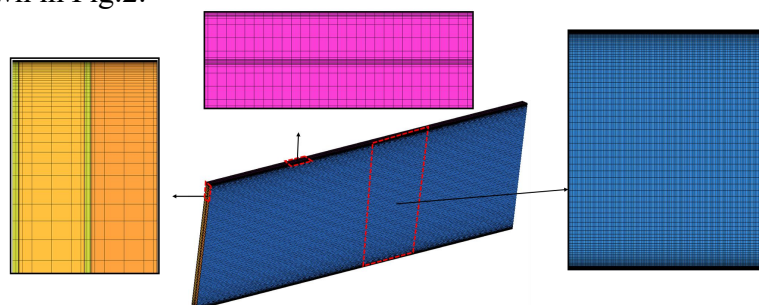


Fig. 2 Straight Plate Section Mesh

In the study of mesh density and computational accuracy, simulations were performed using different mesh counts, including 1.03 million, 1.30 million, 1.85 million, 2.13 million, 2.40 million,

and 2.82 million, with the resulting data illustrated in Fig.3.

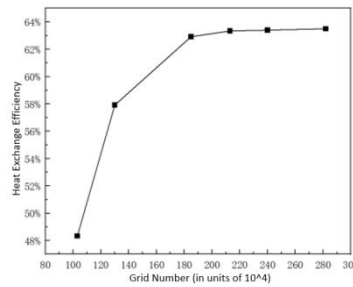


Fig. 3 The Influence of Grid Number on Calculation Results

## 2.2 Mathematical Model and Numerical Method

The fluid flow and conjugate heat transfer within the heat exchanger were analyzed using Computational Fluid Dynamics (CFD), implemented via the CFX solver. The analysis of fluid motion is controlled by the Navier-Stokes (N-S) equations, and the simulation adopts the Ideal Gas Model.

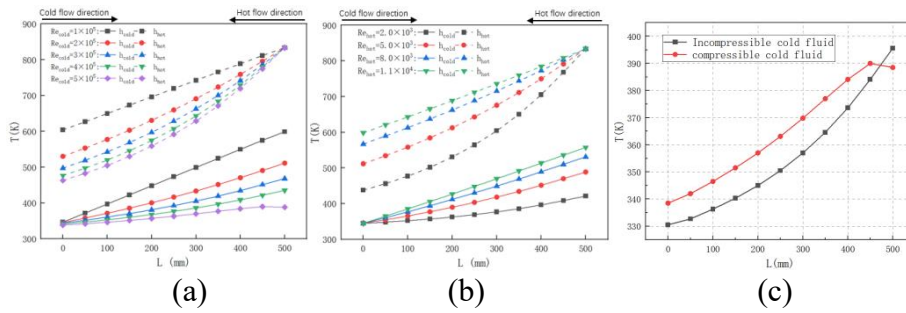
Considering the flow regime specific to the aero-engine system, which is characterized by high velocity and large Reynolds number (Re), the Standard k-epsilon model (a two-equation model under the RANS method) was selected as the turbulence model, as it is suitable for flows at high Re numbers and fully developed turbulence. The fluid property variations were addressed by calculating both viscosity and thermal conductivity using the Sutherland Law, reflecting their dependence on temperature. The fluid domain energy model was set to Total-Energy.

$$\mu = \mu_0 \left(\frac{T}{T_0}\right)^{\frac{3}{2}} \frac{T_0 + S}{T + S} \quad (1)$$

Boundary conditions included applying a no-slip wall condition to all walls. The inlet boundaries were defined by specifying Total Temperature and Total Pressure conditions: the hot side (combustion gas) was set at 834 K and 118280 Pa, and the cold side (ideal gas) was set at 347 K and 176432 Pa. The outlet boundary employed a Mass Flow Outlet condition. For the solid domain, Conjugate Heat Transfer was modeled with Aluminum. The solution utilized a high-resolution scheme.

## 3. Results and Discussion

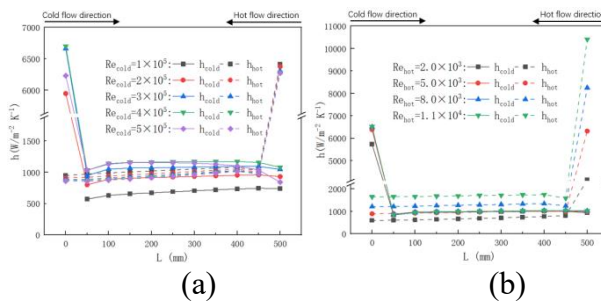
Increasing the cold-side inlet Reynolds number ( $Re_{cold}$ ) significantly enhances the convective heat transfer coefficient of the cold fluid, improving its capacity to absorb heat from the wall and generally lowering the overall temperature levels within the heat exchanger. However, beyond a critical Reynolds number, a notable deceleration in the cold fluid's temperature rise is observed in the downstream section of the flow channel. This temperature stagnation is attributed to a thermodynamic cooling effect caused by the compressibility of the gas. High flow velocities induce a substantial pressure drop along the channel, leading to gas expansion. According to the ideal gas law, this expansion performs work consuming the fluid's internal energy, which generates a cooling effect that partially counteracts the external heating from the walls. Comparative numerical simulations confirmed this mechanism, as incompressible models did not exhibit this phenomenon, thereby isolating gas compressibility as the root cause. Conversely, an increase in the hot-side inlet Reynolds number ( $Re_{hot}$ ) primarily intensifies the heat input per unit time into the system. Unlike the complex compressibility effects observed on the cold side, a higher  $Re_{hot}$  leads to a straightforward increase in fluid temperatures on both the cold and hot sides due to the enhanced thermal energy supply.



(a) Different Cold-side Inlet Reynolds Numbers  
 (b) Different Hot-side Inlet Reynolds Numbers  
 (c) The Influence of Compressibility on Temperature Distribution Along the Flow Path

Fig. 4 Variations of fluid temperature along the channels under different inlet Reynolds Numbers

Fig.5 shows the distribution of convective heat transfer coefficients for cold and hot fluids along the flow direction at different inlet Reynolds numbers. The coefficients on both sides are much higher near the inlet than in the middle and later sections. This occurs because the velocity and thermal boundary layers are not yet fully developed in the inlet region, leading to thinner boundary layers and more effective heat transfer. As flow develops, the boundary layers thicken, causing the heat transfer coefficient to drop rapidly and then stabilize. The inlet effect is limited in scope. Additionally, as the cold-side Reynolds number increases, the cold-side coefficient rises significantly at first, then more slowly, while the hot-side coefficient declines gradually. This is due to increased turbulence and a thinner thermal boundary layer on the cold side, and reduced gas thermal conductivity on the hot side. In contrast, Fig.5(b) shows that a higher hot-side Reynolds number increases the hot-side coefficient due to greater flow velocity, while the cold-side coefficient remains nearly unchanged, indicating weak cross-impact under this heat transfer arrangement.

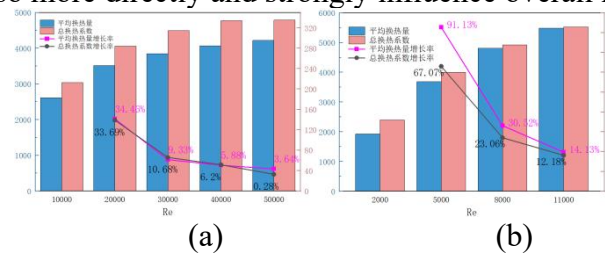


(a) Different Cold-side Inlet Reynolds Numbers  
 (b) Different Hot-side Inlet Reynolds Numbers

Fig. 5 Variation of Fluid Convective Heat Transfer Coefficient Along the Flow Path under Different Inlet Reynolds Numbers

Fig.6 presents the variation in average heat transfer rate and overall heat transfer coefficient of the heat exchanger under different cold-side and hot-side inlet Reynolds numbers. As the cold-side Reynolds number increases, convective heat transfer is enhanced, leading to a gradual rise in both the average heat transfer rate and overall heat transfer coefficient, though the rate of increase slows over time. When the hot-side Reynolds number increases, both the heat input per unit time and the hot-side convective heat transfer intensify, resulting in a significant improvement in both heat transfer metrics. Notably, as the hot-side Reynolds number rises from 2000 to 5000, the average heat transfer rate increases by 91.13%, reflecting high sensitivity to hot-side inlet conditions. A comparison between the figures indicates that while increasing either side's Reynolds number improves heat transfer, the enhancement from raising the hot-side Reynolds number is more pronounced. This suggests that in this configuration, the hot side acts not only as the energy source,

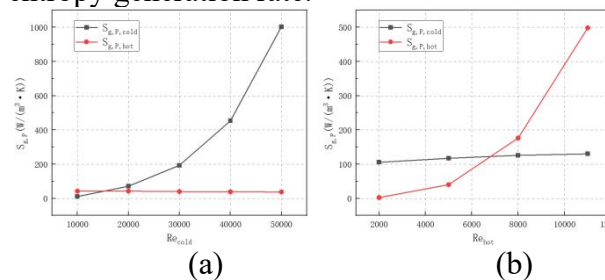
but its flow conditions also more directly and strongly influence overall heat exchange efficiency.



(a) Different Cold-side Inlet Reynolds Numbers  
 (b) Different Hot-side Inlet Reynolds Numbers

Fig. 6 Variations in Average Heat Transfer Rate and Overall Heat Transfer Coefficient of PCHE under Different Inlet Reynolds Numbers

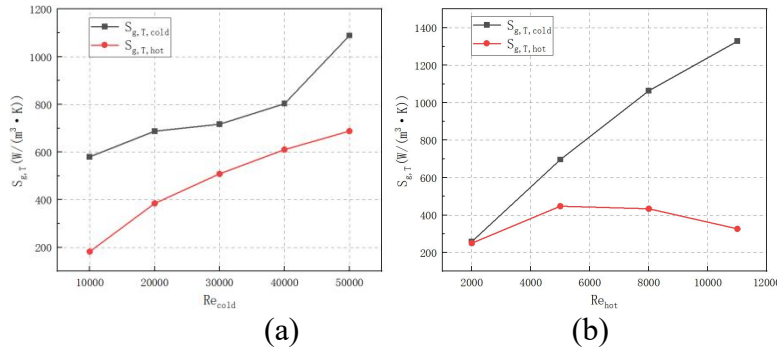
Regarding the flow entropy generation rate ( $S_{g,P}$ ), Fig.7 reveals that as the inlet Reynolds number increases on either the cold or hot side, the flow velocity and turbulent intensity on that side rise. Consequently, the flow entropy generation rate on that side gradually increases, and the magnitude of change progressively enlarges. Comparing Fig7(a) and Fig7(b), it can be seen that when the cold-side inlet Reynolds number increases, the hot-side flow entropy generation rate remains almost unchanged. Conversely, when the hot-side inlet Reynolds number increases, the cold-side flow entropy generation rate gradually increases, and the increase is greater as the hot gas inlet Reynolds number is higher. This is primarily because the physical properties of the cold side are relatively sensitive to temperature: the increase in the hot-side inlet Reynolds number raises the overall temperature of the cold side, leading to a decrease in density and an increase in flow velocity, thus resulting in a higher flow entropy generation rate.



(a) Different Cold-side Inlet Reynolds Numbers  
 (b) Different Hot-side Inlet Reynolds Numbers

Fig. 7 Variations of local flow entropy production rate along the channels under different inlet Reynolds numbers

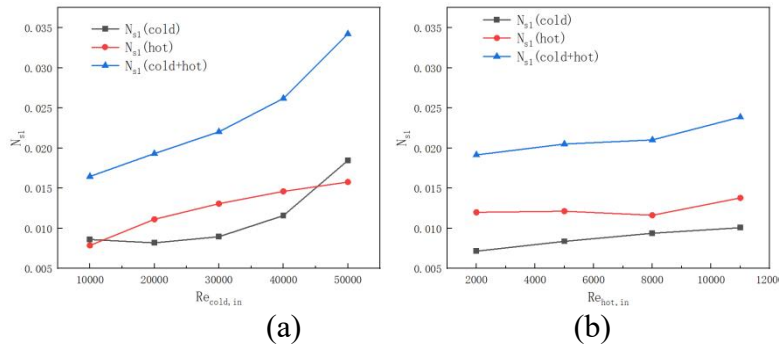
Fig.8 shows that within the  $Re_{cold}$  range of 10,000–50,000, the heat transfer entropy generation rate ( $S_{g,T}$ ) increases monotonically on both the cold and hot sides as the cold-side inlet Reynolds number rises. This trend is attributed to the growing temperature difference between the two channels, as indicated in another figure. Similarly, within the  $Re_{hot}$  range of 2,000–11,000, the cold-side  $S_{g,T}$  continues to rise monotonically with the hot-side Reynolds number. In contrast, the hot-side  $S_{g,T}$  displays non-monotonic behavior: it initially increases from  $Re_{hot} = 2,000$  to 4,000, but then decreases as  $Re_{hot}$  rises further. At lower Reynolds numbers, higher hot-side velocity intensifies heat transfer, raising both the temperature gradient and entropy generation rate. However, once the flow becomes fully turbulent, strong mixing promotes temperature uniformity, reducing the local temperature gradient. Additionally, the earlier onset of a thermally fully developed region stabilizes heat transfer intensity. Together, these effects cause the temperature gradient reduction to dominate, leading to a decline in hot-side  $S_{g,T}$  at higher Reynolds numbers.



(a) Different Cold-side Inlet Reynolds Numbers  
 (b) Different Hot-side Inlet Reynolds Numbers

Fig. 8 Variations of local heat transfer entropy production rate along the channels under different inlet Reynolds numbers

Fig.9 displays the entropy generation number ( $N_{s1}$ ) for the hot side, cold side, and the total system under different inlet Reynolds numbers. As the cold-side Reynolds number rises,  $N_{s1}$  increases on both sides: the cold-side growth accelerates, while the hot-side growth slows gradually, leading to a significant overall increase in total entropy generation. In contrast, Fig.9(a) indicates that increasing the hot-side Reynolds number causes the hot-side  $N_{s1}$  to slightly decrease initially ( $Re_{hot,in} < 8000$ ) and then rise noticeably beyond  $Re_{hot,in} = 8000$ . Meanwhile, the cold-side  $N_{s1}$  consistently increases, resulting in an overall growth in system entropy generation. A comparison shows that the cold-side Reynolds number has a much stronger influence on entropy generation across all components than the hot-side Reynolds number. This suggests that adjusting the cold-side flow offers more sensitive control and greater optimization potential for enhancing heat exchanger performance.



(a) Different Cold-side Inlet Reynolds Numbers  
 (b) Different Hot-side Inlet Reynolds Numbers

Fig. 9 Overall entropy production of fluid at different inlet Reynolds numbers

#### 4. Summary

This study performed a systematic numerical investigation into the thermofluidic performance and thermodynamic irreversibility of an annular plate heat exchanger for micro aero-engines, considering the effects of high-Mach number compressible flow. The major conclusions are drawn as follows:

**Compressibility-Induced Expansion Cooling:** A unique heat transfer mechanism was identified under high-speed flow conditions. As the cold-side Reynolds number ( $Re_{cold}$ ) increases, the convective heat transfer coefficient improves significantly. However, beyond a critical threshold, the significant pressure drop induces gas expansion, generating a thermodynamic cooling effect that suppresses the fluid temperature rise in the downstream section. This mechanism was explicitly validated by contrasting compressible and incompressible flow models.

**Dominance of Hot-side Reynolds Number:** The hot-side Reynolds number ( $Re_{hot}$ ) acts as the

dominant factor for the total heat exchange capacity. Increasing  $Re_{hot}$  from 2000 to 5000 results in a 91.13% surge in the average heat transfer rate, indicating that enhancing the hot-side flow condition is the most direct pathway to boosting power output.

**Entropy Generation and Optimization:** The thermodynamic analysis reveals that the cold-side Reynolds number is more sensitive to the system's total entropy generation number ( $Ns_1$ ) than the hot side. While the hot-side heat transfer entropy generation exhibits non-monotonic behavior due to the interplay between turbulent mixing and temperature gradients, the cold side shows a consistent increase. Consequently, controlling  $Re_{cold}$  specifically keeping it within the optimal range identified.

In conclusion, this work clarifies the conflict between heat transfer enhancement and flow loss in high-speed micro-recuperators, providing theoretical guidelines for optimizing the trade-off between thermal efficiency and entropy generation in next-generation aviation power systems.

## References

- [1] Suresh, S., & Subhash, K. (2018). Recuperators for micro gas turbine engines: A review of design and performance challenges. *Applied Thermal Engineering*, 137, 725-739.
- [2] Xu, Z., Xu, S., & Sundén, B. (2020). Numerical analysis of heat transfer enhancement and pressure drop in minichannels with pin fins under high Reynolds number. *International Journal of Heat and Mass Transfer*, 149, 119208.
- [3] Michna, G. J., Garimella, S. V., & Witte, M. M. (2007). Effect of Reynolds number on the friction factor and flow characteristics in corrugated channels. *International Journal of Heat and Mass Transfer*, 50(9-10), 1719-1730.
- [4] Bejan, A. (1996). Entropy generation minimization: The new thermodynamics of finite-size devices and finite-time processes. *Journal of Applied Physics*, 79(3), 1191-1218.
- [5] Shah, R. K., & Sekulić, D. P. (2003). *Fundamentals of heat exchanger design*. John Wiley & Sons.